Green and Orange CdTe Quantum Dots as Effective pH-Sensitive Fluorescent Probes for Dual Simultaneous and Independent Detection of Viruses

Zhengtao Deng,[†,§,||] Yun Zhang,[†,#] Jiachang Yue,[*,‡] Fangqiong Tang,[*,§] and Qun Wei[⊥]

The National Laboratory of Biomacromolecules, Institute of Biophysics, Chinese Academy of Sciences, Beijing 100101, China, Technical Institute of Physics and Chemistry, Chinese Academy of Sciences, Beijing 100080, China, Graduate School of Chinese Academy of Sciences, Beijing 100080, China, School of Life Science and Technology, Xi′an Jiaotong University, Xi′an 710049, China, and Department of Biochemistry and Molecular Biology, Beijing Normal University, Beijing Keb Laboratory, Beijing 100875, China

Received: June 14, 2007; In Final Form: August 1, 2007

One of the most highlighted and fastest moving interfaces of nanotechnology is the application of quantum dots (QDs) in biology. The unparalleled advantages of the size-tunable fluorescent emission and the simultaneous excitation at a single wavelength make QDs the great possibility for use in optical encoding detection. In this paper, we report that green and orange CdTe QDs as convenient, cheap, reversible, and effective pH-sensitive fluorescent probes could monitor the proton (H^+) flux driven by ATP synthesis for dual simultaneous and independent detection of viruses on the basis of antibody−antigen reactions. A new kind of biosensor (consisting of the mixture of green-QDs-labeled chromatophores and orange-QDs-labeled chromatophores) fluorescent measurement system was established for rapid, simultaneous, and independent detection of two different kinds of viruses (i.e., H9 avian influenza virus and MHV68 virus). It is crucial to find that the green and orange QDs labeled biosensors coexisting in the detection system can work independently and do not interfere with each another in the fluorescence assays. In addition, a primary steady electric double layer (EDL) model for the QDs biosensors was proposed to illustrate the mechanism of simultaneous and independent detection of the biosensors. We believe that the pH-sensitive CdTe QDs based detection system, described in this paper, is an important step toward optical encoding and has a great potential for simultaneous and independent qualitative and quantitative multiple detection systems.

Introduction

In the past few years, one of the most highlighted and fastest moving interfaces of nanotechnology is the application of semiconductor quantum dots (QDs) in life science research by using them as novel fluorescent probes in biological detection.[1−10] QDs provide many advantages over traditional organic dyes: high quantum yield, high molar extinction coefficients, broad absorption with narrow, symmetric photoluminescence (PL) spectra spanning the UV to near-infrared, high resistance to photobleaching, and exceptional resistance to photodegradation and chemical degradation.[3−8] More importantly, the unparalleled ability for size-tunable fluorescent emission as a function of core size and the broad excitation spectra, which allow excitation of mixed QDs populations at a single wavelength far removed, make them a great possibility for use in optical encoding detection.[9−11] In 1998, both Alivisatos' and Nie's groups reported the first use of colloidal CdSe QDs for biological labeling.[1,2] Since then, the CdSe QDs have been the most popular QDs in biological detection, which consist of a CdSe core, followed by a ZnS shell and one or more organic coats to make them water-soluble.[6−15] The present synthetic process for CdSe QDs has several shortcomings: It is time- and cost-consuming, complicated, and conducted at high temperature (200−300 °C);[16−17] in addition, the surface exchange of QD primary ligands (such as trioctylphosphine oxide (TOPO) or hexadecylamine (HAD)) and subsequent transfer in aqueous solutions results in a significant loss of their PL properties.[18−20] Thiol-modified CdTe QDs are a very promising alternative to

SCHEME 1: Illustration of BPCL-III Fluorescent Measurement System[a]

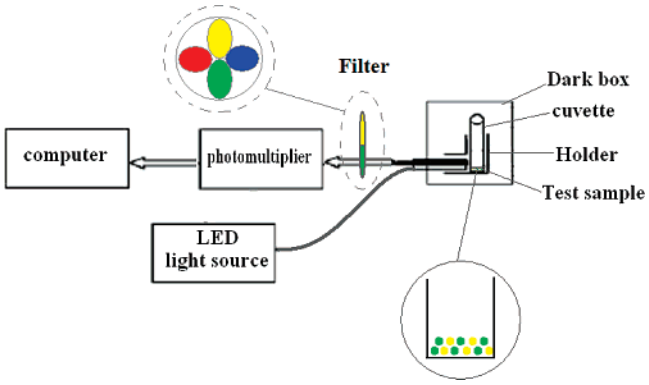

[a] QD biosensors are excited by light-emitting diode (LED, with wavelength at 470 nm). The photoluminescence signals of the QD biosensors will go through the filter, be amplified by the photomultiplier, and be recorded by computer.

* Corresponding authors. Phone: 86-10-64888576 (J.Y.); 86-10-82543521 (F.T.). Fax: 86-10-64871293 (J.Y.); 86-10-62554670 (F.T.). E-mail: yuejc@sun5.ibp.ac.cn (J.Y.); tangfq@mail.ipc.ac.cn (F.T.).
† These authors contributed equally to this work.
§ Technical Institute of Physics and Chemistry, Chinese Academy of Sciences.
|| Graduate School of Chinese Academy of Sciences.
‡ Institute of Biophysics, Chinese Academy of Sciences.
⊥ Beijing Normal University.
School of Life Science and Technology, Xi′an Jiaotong University.

10.1021/jp074609z CCC: $37.00
Published on Web 09/21/2007

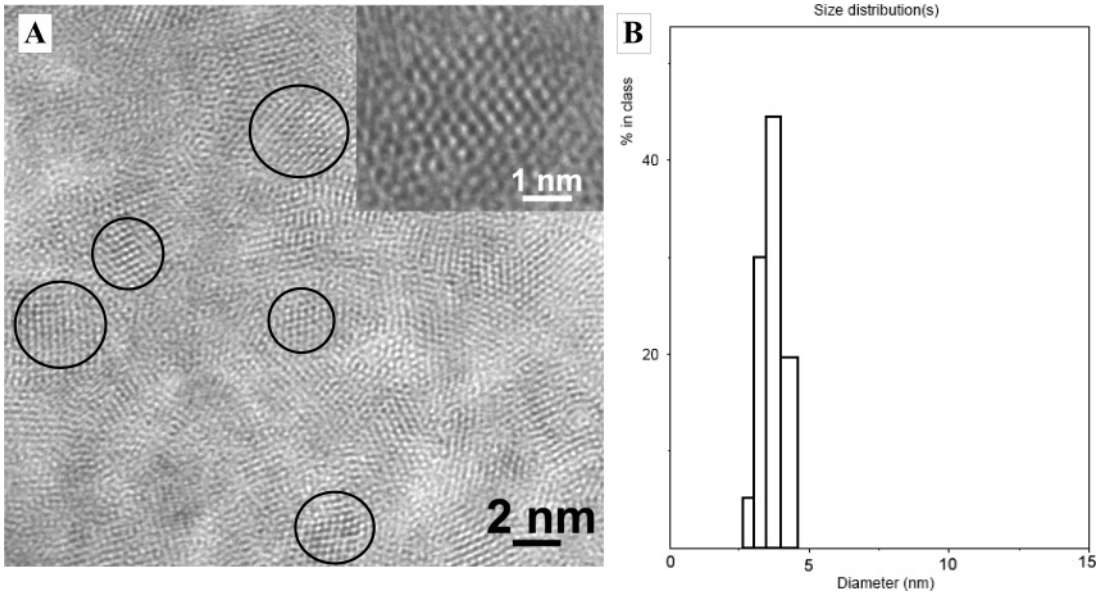

Figure 1. (A) High-resolution transmission electron microscopy (HRTEM) image of the pH-sensitive orange CdTe QDs with emission wavelength at 585 nm. (B) The dynamic light scattering (DLS) analysis of the same orange CdTe QDs. The cycles in A marked out several individual QD. Inset A, the enlarged image of a single QD.

CdSe QDs, because they can be directly synthesized in water with high quantum yield and size-tunable fluorescent emission at low temperature (80−100 °C) and easily modified by biomolecules (such as thiolglycolic acid (TGA) and L-CYSTEINE (L-cys)) during the synthesis process.[21−23] More importantly, it was reported that TGA modified CdTe QDs in solution were pH-sensitive without any additional treatment,[21] while, for CdSe, making pH-sensitive sensors was much difficult, for example, using complex fluorescence resonant energy transfer (FRET) between the emissive CdSe/ZnS QDs and dyes conjugated to the QDs surface have been reported recently.[24−25] It is expected that the CdTe QDs have a great potential to be used as convenient, cheap, reversible, and effective pH-sensitive fluorescent probes for application in pH meter and in multiplex biological detection.

Proton is a strong acidic species, and it interacts with basic groups of biomolecules.[26] Proton transfer is important both for many enzyme reaction mechanisms and proton pumping across membranes.[26] The F_0F_1-ATP synthase is a nanoscale rotary biological motor. Because of its transduction of energy, nanoscale size, and possible practicability in nanotechnology, many scientists have attempted to develop the motor as a new generation of biosensor.[27] For example, Cui et al.[28] have labeled fluorescein-DHPE (F-DHPE) on the surface of chromatophores to detect proton flux through F_0F_1-ATPase driven by ATP hydrolysis. On the basis of their experiment, we developed a new biosensor, using F1300 as a pH-sensitive probe, to detect a single virus.[29] Recently, we have used single-color CdTe QDs to replace organic dyes, i.e., F1300, as the proton sensor, which were labeled on the surface of chromatophores to construct a single-color QD biosensor.[30] It was demonstrated that the CdTe QDs are the ideal alternatives to the organic dyes due to their effective pH-sensitive fluorescent emission, high quantum yield, and exceptional resistance to photodegradation and chemical degradation over long periods of time.[30] It is generally expected that the unparalleled ability of the size-tunable fluorescent emission and the simultaneous excitation of mixed QDs populations at a single wavelength make QDs the great possibility for using in optical encoding detection. A few examples have been reported for the QDs-related optical encoding. For example, Han et al. have developed a flexible method of multicolor optical encoding by embedding different-sized CdSe/ZnS QDs into polymeric microbeads.[31] However, it is still a great challenge to realize the multiplex biological detection based on multicolor QDs besides the polymeric microbeads method.

In this paper, we developed a new kind of QDs-based biosensor, consisting of mixtures of green-QDs-labeled chromatophores and orange-QDs-labeled chromatophores, to detect different kinds of viruses. A new virus detection system has been established for rapid, simultaneous, and independent detection of H9 avian influenza virus and MHV68 virus simultaneously and independently. It was found that the green- and orange-QDs-labeled biosensors coexisting in one virus-detection system can work independently and do not interfere with each other in the fluorescence assays. In addition, a primary steady electric double layer (EDL) model was proposed to explain the mechanism of simultaneous and independent detection of the biosensors. The pH-sensitive QDs-based detection system described in this paper is expected to be an indispensable step toward optical encoding and has a great potential for simultaneous and independent quantitative and qualitative multiple detection systems.

Experimental Section

Preparation of pH-Sensitive CdTe QDs. The CdTe QDs were synthesized via a modified protocol, which was adopted from the literature,[21−23] i.e., adding freshly prepared NaHTe solution to N_2-saturated $Cd(NO_3)_2$ solutions at pH 8.5 in the presence of thiolglycolic acid (TGA) as a stabilizing agent. The molar ratio of Cd^{2+}/TGA/HTe^- was fixed at 1:2:0.5. A small amount of ammonia was added in the solution as the additional stabilizing agent and pH-controller, which would enable us to obtain high-quality QDs with small size and high quantum yield. A series of QDs with their size ranging from 2.0 to 6.0 nm were obtained. In this work, we used the QDs with maximum emission wavelength at 535 nm (green) and 585 nm (orange).

Preparation of QDs Labeled Chromatophores. Chromatophores were prepared from the cells of *Rhodospirillum rubrum* according to refs 32 and 33. The suspension of chromatophores (100 μL) was washed by centrifugation at 13 000 rpm for 30

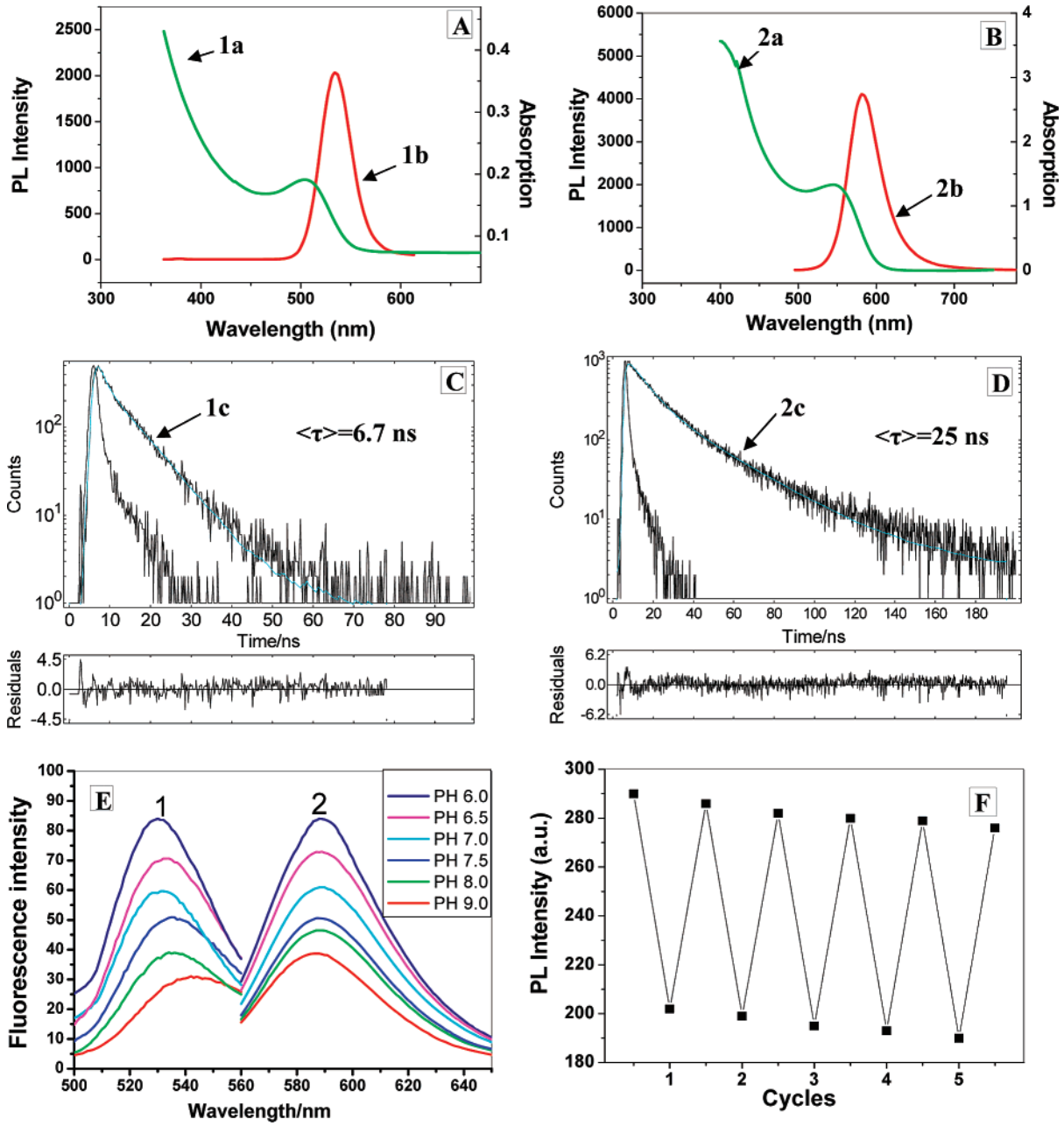

Figure 2. Optical properties of QDs with emission wavelength at 535 nm for "1" and at 585 nm for "2", respectively: (A, B) UV−vis absorption (1a, 2a) and photoluminescence emission spectra (1b, 2b) of the QDs. (C, D) Time decay of the light emissions monitored at their maximum emission (1c, 2c) of the QDs. (E) Photoluminescence spectra of CdTe QDs at various pH values. (F) PL intensity of the CdTe QDs reversibly goes upward and downward by alternating the pH value of the buffer. One cycle means that the fluorescent intensity is measured as the value is changed from pH 6 to 9 and then from pH 9 to 6.

min at 4 °C to wash the glycerol away. The precipitate was resuspended in buffer A (50 mM Tricine-NaOH, 5 mM $MgCl_2$, 10 mM KCl, pH 6.5) and incubated for 3 h at room temperature after adding 100 μL of CdTe QDs (about $1 \times 10^{15}/\mu$L (see Supporting Information), dissolved in water). Free QDs were washed away three times by centrifugation at 13 000 rpm for 30 min at 4 °C. The precipitate (QD-labeled chromatophores) was resuspended in 100 μL of 50 mM Tricine buffer (pH 6.5) and stored at 4 °C before usage.

Preparation of Viruses and Antibodies. The H9 influenza A and H9 influenza A antibodies were obtained from Dr. Z. Q. Ni (Harbin Veterinary Research Institute). Murine herpesvirus68 (MHV68) were inactivated at 60 °C/30 min, and MHV68 antibody were provided by Professor H. Y. Deng (Center for Infection and Immunity, Institute of Biophysics, CAS).

Preparation of β-Subunit Antibody Labeled with Biotin-Streptavidin and H9 Avian Influenza Virus Antibody (or MHV68 Antibody) Labeled with Biotin. The β-subunit of F_0F_1-ATPase was isolated from thermophilic bacterium Bacillus PS3 (TF1β) expressed in *Escherichia coli* JM103 according to ref 34 and purified according to ref 35. The antibody was prepared according to ref 36 and purified by precipitation with $(NH_4)_2SO_4$ (33 wt % in water). Furthermore biotin was incubated with β-subunit antibody (mol/mol, 3/1) at room temperature for 30 min and then was incubated with streptavidin (mol/mol, 1/1) at room temperature for 30 min. The H9 avian influenza virus antibody (or MHV68 antibody) with biotin (mol/mol, 1/3) was incubated at room temperature for 30 min.

Construction of QDs-Biosensors. Green CdTe QD chromatophores biosensors were incubated with β-subunit antibody

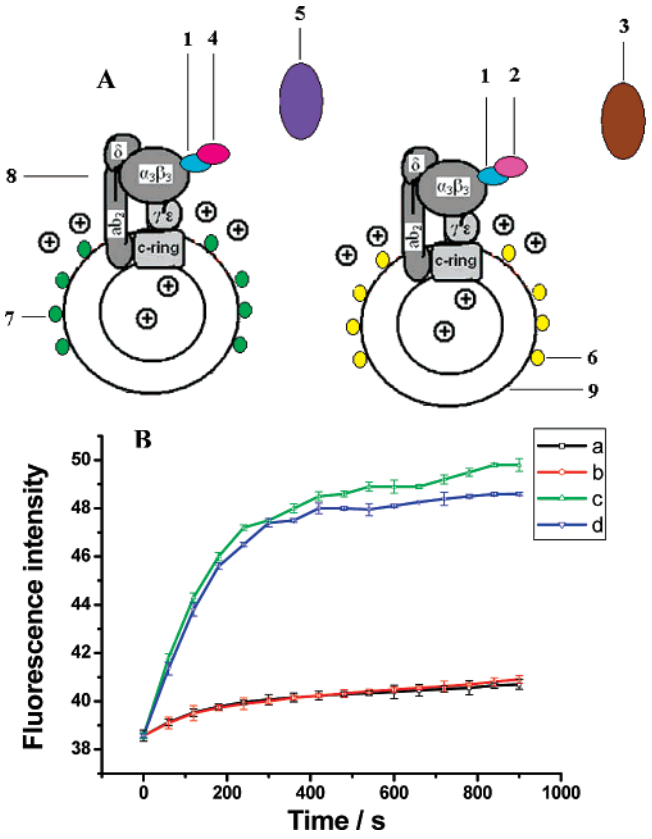

Figure 3. (A) Basic design of QD biosensors based on F_0F_1-ATPase: (1) antibody of β-subunit; (2) the antibody of MHV68; (3) MHV68; (4) the antibody of H9 avian influenza virus; (5) H9 avian influenza virus; (6) CdTe QDs with emission wavelength at 585 nm; (7) CdTe QDs with emission wavelength at 535 nm; (8) F_0F_1-ATPase within chromatophores; (9) chromatophores. (B) Changes of fluorescence intensity of QD biosensors with and without viruses. Curve a: The changes of fluorescence intensity of orange QD biosensors without MHV68 when the ADP is added to initialize reaction. Curve b: The changes of fluorescence intensity of green QD biosensors without H9 avian influenza virus when the ADP is added to initialize reaction. Curve c: The changes of fluorescence intensity of orange QD biosensors with capturing MHV68 when the ADP is added to initialize reaction. Curve d: The changes of fluorescence intensity of green QD biosensors with capturing H9 avian influenza virus when the ADP is added to initialize reaction.

(mol/mol, 1/3), which were labeled with biotin−streptavidin, for 60 min at room temperature, and washed three times by centrifugation at 13 000 rpm for 30 min; then biotin-labeled H9 avian influenza virus antibody (mol/mol, 1/5) was added at room temperature for 10 min. The free fraction was washed by centrifugation. Similarly, the orange CdTe QD chromatophores biosensors were incubated with β-subunit antibody (mol/mol, 1/3), which were labeled with biotin−streptavidin, for 60 min at room temperature and washed three times by centrifugation at 13 000 rpm for 30 min; then biotin-labeled MHV68 antibody (mol/mol, 1/5) was added at room temperature for 10 min. The free fraction was also washed by centrifugation. The prepared QD biosensors were stored at 4 °C before usage.

Fluorescence Assay. The fluorescence spectra of CdTe QDs were measured by common fluorescence instrument. The fluorescence intensities of CdTe QD biosensors in the cuvette were measured by the BPCL-III (see Scheme 1, manufactured at the Institute of Biophysics, CAS, designed by Professor Z. L. Zhang). The ATP synthesis buffer (0.1 mM Tricine, pH 8.5, 5 mM $MgCl_2$, 5 mM K_2HPO_4, and 10% glycerol, ADP 2 mM) was added to initialize ATP synthesis by F_1F_0-ATPase. The fluorescence intensities of CdTe QD biosensors were excited at 470 nm with the usage of filters (535 ± 10 nm and 585 ± 10 nm, respectively), and recorded at 37 °C. All experimental data were calculated from four to six independent tests.

Instruments. The high-resolution transmission electron microscopy (HRTEM) and the selected area electron diffraction (SAED) pattern were performed on a JEOL JEM-2010 electron microscope operating at 200 kV. The dynamic light scattering (DLS) analysis was measured by Malvern zetasizer 3000HS. The X-ray powder diffraction (XRD) measurement was employed a Japan Regaku D/max γA X-ray diffractometer equipped with graphite monochromatized Cu Kα radiation (λ = 1.5418 Å) irradiated with a scanning rate of 0.02 deg/s. The ultraviolet and visible absorption (UV−vis) spectra were recorded with a JASCO 570 spectrophotometer at room temperature. The PL spectra were measured with a Hitachi F4500 fluorescence spectrophotometer at room temperature. The fluorescence decay processes were recorded with time-correlated single-photon counting (TCSPC) technique on an Edinburgh FLS920 phosphorescence lifetime system at room temperature.

Results and Discussion

Characterization and Optical Properties of the pH-Sensitive CdTe QDs. Figure 1A shows the typical HRTEM image of the pH-sensitive CdTe QDs with the emission peak at 585 nm. The existence of lattice planes on the HRTEM confirms the good crystallinity of the sample. The dynamic light scattering (DLS) of the TGA−CdTe QDs in aqueous solution reveals that the QDs have a narrow size distribution with an average size of 3.8 nm (see Figure 1B). The powder XRD pattern of the CdTe QDs (see Figure S1) has characteristic features matching the bulk cubic CdTe pattern. These diffraction features appearing at about 24.1, 39.7, and 46.9° correspond to the (111), (220), and (311) planes of the zinc blende phase of CdTe (Joint Committee on Powder Diffraction Standards file No. 75-2086), respectively. The selected area electron diffraction (SAED) pattern of about 20 CdTe QDs (inset Figure S1 of the Supporting Information) can also be indexed to the cubic phase of CdTe.

Figure 2 shows the optical properties of pH-sensitive CdTe QDs, such as the UV−vis absorption spectra, the photoluminescence emission spectra, the time−decay curves, and the pH-dependent photoluminescence spectra. The obvious UV−vis absorption peaks indicate that the CdTe QDs are close to monodispersed. Parts A and B of Figure 2 show that photoluminescence emission maximum appears at 535 nm for green QDs and at 585 nm for orange QDs, respectively. The photoluminescence full width at half-maximum (fwhm) are about 36 nm for green QDs and 48 nm for orange QDs, respectively. The photoluminescence quantum yield (PL QY) is about 32% for green CdTe QDs and about 37% for orange CdTe QDs, respectively, using a conventional route according to ref 23. The room-temperature time−decay curve of the QDs with an emission at 535 nm fits well to a biexponential function with a fast part of 1.275 ns (28.59%) and a slow part of 7.074 ns (71.41%), and the calculated average decay time is 6.7 ns; while for the QDs with an emission at 585 nm, it fits well to a biexponential function with a fast part of 7.610 ns (42.19%) and a slow part of 28.47 ns (57.81%), and the calculated average decay time is 25 ns. The time−decay curves of the QDs are similar to the highly luminescent CdTe QDs prepared in TOP/DDA (trioctylphosphine/dodecylamine) and transferred into water by using an aminoethanethiol·HCl (AET) or mercaptopropionic acid (MPA).[38]

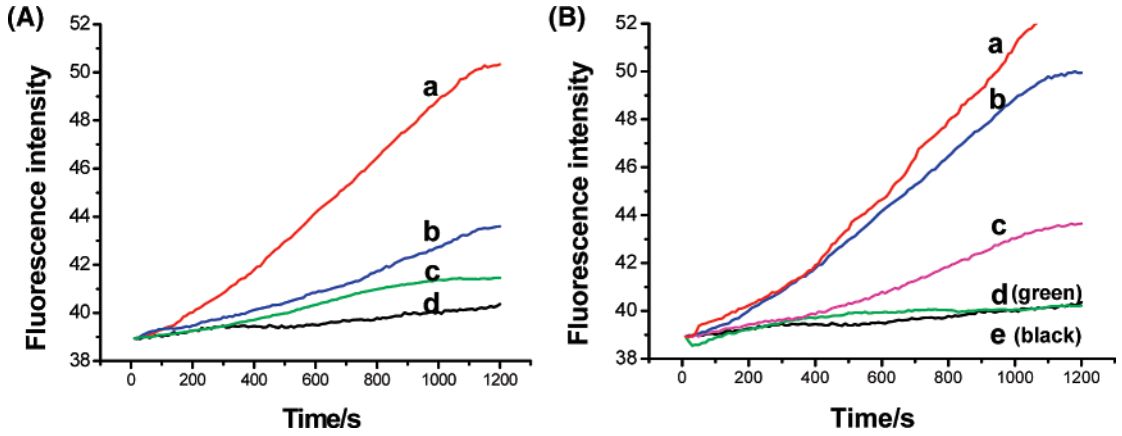

Figure 4. (A) Effect of dose of H9 avian influenza virus: Green QD biosensors are loaded by H9 avian influenza virus (a) diluted 100 times, (b) diluted 500 times, and (c) diluted 1000 times; (d) green QDs-biosensors are loaded without H9 avian influenza virus as control. (B) Effect of time course of H9 avian influenza virus incubated with green QDs-biosensors: Green QD biosensors are loaded by H9 avian influenza virus (a) diluted 100 times for 60 min incubation, (b) diluted 100 times for 30 min incubation, (c) diluted 100 times for 10 min incubation, and (d) diluted 100 times for 3 min incubation; (e) green QD biosensors without adding H9 avian influenza virus as control.

The pH sensitivity of the green and orange CdTe QDs is investigated by dissolving them in buffers with different pH, i.e., 6.0, 6.5, 7.0, 7.5, 8.0, and 9.0, respectively. The solution is excited at 470 nm, and the PL spectra are shown in Figure 2E. It is found that, for CdTe QDs, both free-standing in solution and labeled on the chromatophores, the PL intensity increases monotonically with decreasing of pH value, exhibiting a very good sensitivity to pH value. The PL intensity of CdTe QDs is pH-dependent, suggesting application of these QDs as pH sensors. Since the molar ratio of Cd^{2+}/TGA/HTe^- is fixed at 1:2:0.5 in our preparation, Cd−TGA complexes are formed in the solution. It has been demonstrated that cadmium and TGA can form different polynuclear complexes in water and that the formation of Cd−TGA complexes strongly depends on the pH value.[21] When the pH value is decreased from 9.0 to 6.0, more free TGA and Cd^{2+} will be released from the Cd−TGA complexes. Therefore, more trap sites on the CdTe surface will be removed, thus dramatically improving the fluorescence efficiency. In addition, as the pH value is decreased from 9.0 to 6.0, the PL peak is shifted a little. It is supposed that the shift is attributed to the additional sulfuration reaction, which takes place on the CdTe surface during the decrease of the pH value, similar to the reported results.[21,39,40] It's worth pointing out that although the peak positions are a little variable depending on the pH value, it does not interfere with the detection of the viruses in the present strategy. Figure 2F demonstrates the reversibility of the fluorescence changes. Green CdTe QDs are used as an example. The pH value is changed from 6.0 to 9.0 and again to 6.0, and the fluorescence intensity is measured at each pH value. This cycle is repeated 5 times. The results indicate that the changes in the fluorescence intensity are reversible. It is also found that CdTe QDs labeled on chromatophores are stable more than 1 month at 4 °C. All the above experimental results reveal that the highly luminescent pH-sensitive CdTe QDs can be the excellent candidates for fluorescent probes.

Building of QD Biosensors. As shown in Figure 3A, green and orange CdTe QDs are used as the pH sensors labeled on chromatophores to construct the QD biosensors, which is the basic design of QD biosensors. When ADP is added to initialize the reaction, protons are pumped out of the chromatophores, resulting in the fluorescent intensity change of CdTe QDs, while the rate of the fluorescent intensity change reveals the activity of ATP synthetase. On the basis of this mechanism, when the antibody (labeled on the β-subunit) captures virus, there exists a positive influence on the β-subunit, which enhances the ATPsynthetase activity, and we can obtain a faster fluorescent intensity change. Therefore, the ATPsynthetase can be used as a virus detector by measuring the rate of QDs' fluorescent intensity changes. Although the exact mechanism of virus activation of ATPsynthetase is still under discussion, the QD biosensor for virus detection is primarily achieved. Furthermore, green and orange CdTe QDs can be used as dual pH sensors labeled on chromatophores to construct the mixed QD biosensors. When orange QD biosensors capture MHV68, the fluorescent intensity change is faster than that without MHV68 (Figure 3B curve c vs curve a); while when green QD biosensors capture H9 avian influenza virus, the fluorescent intensity change is faster than that without capturing H9 avian influenza virus (Figure 3B curve d vs curve b).

The green QD biosensors are taken as an example for further dose effect of the H9 virus test, as shown in Figure 4A. The average rate of fluorescent change is estimated to be 0.55 (curve a), 0.24 (curve b), and 0.13 unit/min (curve c), when the concentration of virus was 90, 18, and 9 particles/μL, respectively. Furthermore, the time-course changes are shown in Figure 4B. It is revealed that the rate of changes of fluorescence intensity are about 0.73, 0.54, 0.24, 0.07, and 0.07 unit/min for the incubation of 60, 30, 10, 3, and 0 min, respectively. These results indicate that the QD biosensors might be a novel virus detector with high sensitivity to very low virus concentration.

Application of QDs-Biosensors in Detection of Viruses. As shown in Scheme 1, the QD-biosensors system is established, where the green QD biosensors mixed with the orange QD biosensors. Figure 5 shows the usage of the mixed QD-biosensors system for virus detection. When the H9 virus is loaded, the fluorescent intensity at 535 nm increases rapidly (Figure 5A, curve a), due to the fact that the green QD biosensors are labeled with H9 virus antibody, and the antibody−antigen reaction enhances the activity of the ATPsynthetase. While the MHV68 is loaded, the fluorescence intensity at 585 nm will increase rapidly (Figure 5B, curve b), due to the enhancement of the activity of the ATPsynthetase of the orange QD biosensors. Furthermore, when the H9 virus and MHV68 are loaded together, both the fluorescent intensities at 535 and at 585 nm are changes rapidly (Figure 5C, curves a and b). The results indicate that each part of the QD biosensors can work independently and do not interfere with each another in the fluorescence assays.

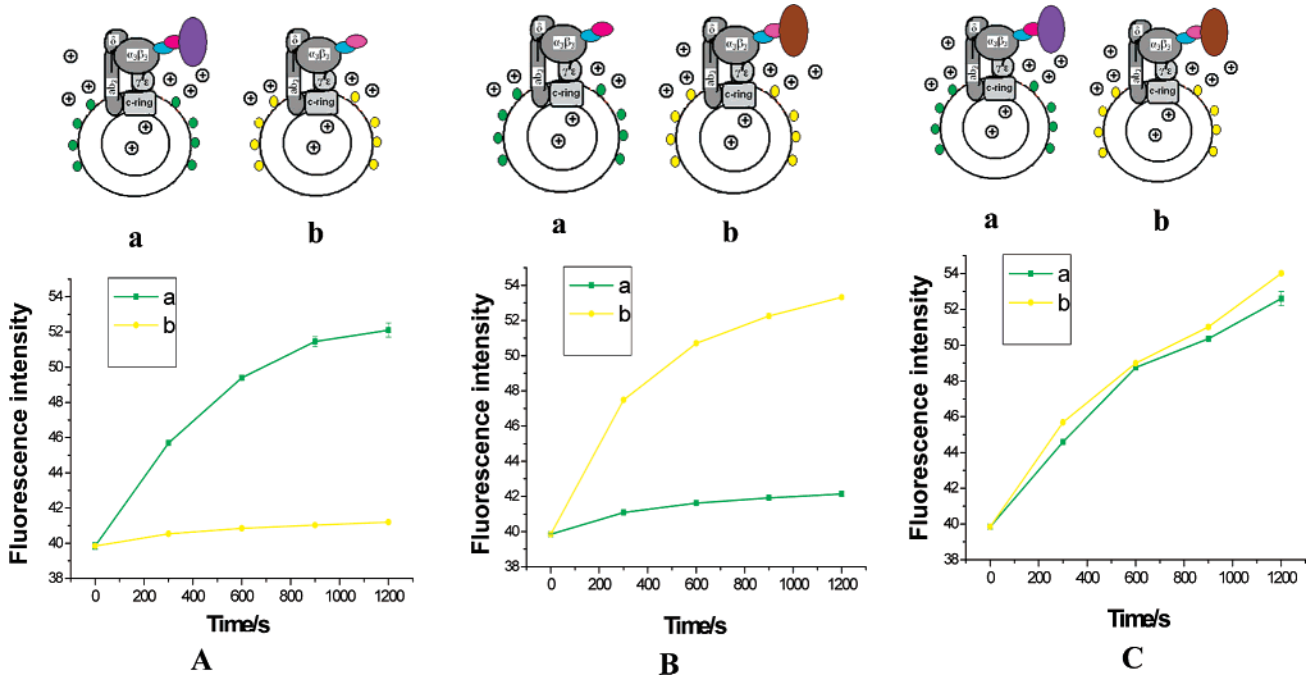

Figure 5. Detection of viruses by the QDs-biosensors. (A) H9 avian influenza virus detected by the QD biosensors: (a) QD biosensors (emission at 535 nm) loaded by antibodies (antibody of β-subunit and second antibody of H9 avian influenza virus) with capture of H9 avian influenza virus; (b) QD biosensors (emission at 585 nm) loaded by antibodies (antibody of β-subunit and second antibody of MHV68). Schematic illustrations are shown in insets a and b. (B) MHV68 detected by the QDs-biosensors: (a) QD biosensors (emission at 535 nm) loaded by antibodies (antibody of β-subunit and antibody of H9 avian influenza virus); (b) QD biosensors (emission at 585 nm) loaded by antibodies (antibody of β-subunit with antibody of MHV68) with capture of MHV68. Schematic illustrations are shown in insets a and b. (C) H9 avian influenza virus and MHV68 detected by the QD biosensors simultaneously and independently: (a) QD biosensors (emission at 535 nm) loaded by antibodies (antibody of β-subunit and antibody of H9 avian influenza virus) with capture of H9 avian influenza virus; (b) QD biosensors (emission at 585 nm) loaded by antibodies (antibody of β-subunit and antibody of MHV68) with capture of MHV68. Schematic illustrations are shown in insets a and b.

As seen in Figure 6, the above results are clearly shown in a histogram. Columns a and b represent the QD biosensors without capturing any viruses as control. When the H9 virus is loaded, the fluorescent intensity increases markedly at 535 nm and a little enhancement is detected at 585 nm (columns c and d); when the MHV68 is loaded, there is a little increased at 535 nm, but markedly increased at 585 nm (columns e and f); when H9 and MHV68 are loaded, both of them increase (columns g and h). On the basis of these results, the independence of each part of the QD biosensors is tested, and the independence will offer us an opportunity to develop an optical coding method applied in mass viruses detection.

Steady Electric Double Layer Model of the QD Biosensors. As it is mentioned above, the green and the orange QD biosensors in one system can work independently and do not interfere with each another in the fluorescence assays, which is very important for application in the multiplex viruses detection. The primary mechanism could be explained as follows by a classical steady EDL model, which describes the variation of electric potential near a surface and has a large bearing on the behaviors of colloids and other surfaces in contact with solutions.[41−43] Figure 7 illustrates the microenvironments of CdTe QDs on the surface of chromatophores in response to proton transfer. Figure 7A shows the EDL model of green QD biosensors with the absorbed layer and the diffused layer. When ADP initialized the ATP synthesis reaction, protons are pumped out of chromatophores (arrow 1) and retained in the absorbed layer, resulting in the fluorescent intensity change of QDs. It is worth pointing out that the protons diffused into the diffused layer (arrow 2) and subsequently into the solution (arrow 3) are negligible due to the electric repulsion effect. In the same time, the protons diffused from the solution into the diffused layer (arrow 4) and subsequently into absorbed layer (arrow 5)

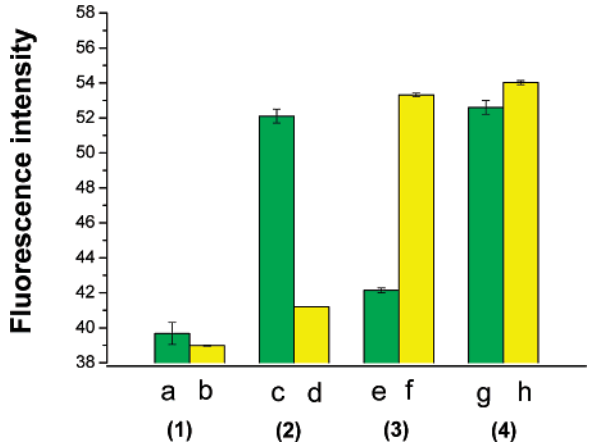

Figure 6. Data of QD biosensors in detection of viruses. Group 1 control: (a) Green QD chromatophores loaded by first antibody of β-subunit and second antibody of H9 avian influenza virus; (b) orange QD biosensors loaded by first antibody of β-subunit and second antibody of MHV68. Group 2 after incubation with H9 virus: (c) Green QD biosensors loaded by first antibody of β-subunit and second antibody of H9 avian influenza virus; (d) orange QD biosensors loaded by first antibody of β-subunit and second antibody of MHV68. Group 3 after incubation with MHV68: (e) Green QD biosensors loaded by first antibody of β-subunit and second antibody of H9 avian influenza; (f) orange QD biosensors loaded by first antibody of β-subunit and second antibody of MHV68. Group 4 after incubation with the mixture of H9 virus and MHV68: (g) Green QD biosensors loaded by first antibody of β-subunit and second antibody of H9 avian influenza virus; (h) orange QD biosensors loaded by first antibody of β-subunit and second antibody of MHV68. All experimental data are based on four to six independent tests.

are also negligible, as shown in the ELD model of orange QD biosensors (Figure 7B). Therefore, the protons pumped out of

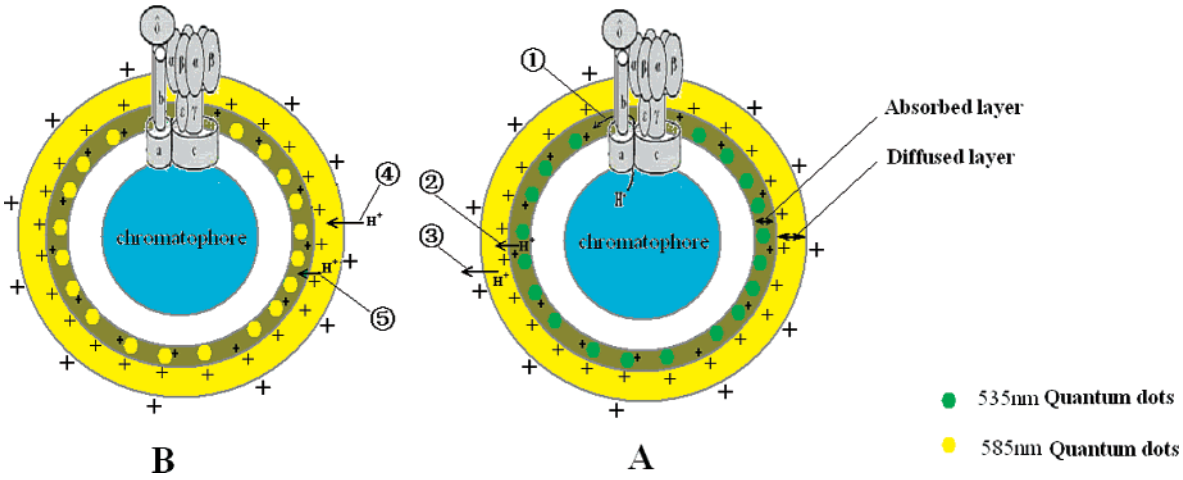

Figure 7. Schematic illustration of the electric double layers model of the microenvironment of CdTe QDs labeled on the surface of chromatophores. During ATP synthesis, arrow 1 shows the proton transfer from inside to the absorbed layer, arrow 2 shows the protons diffusing from the absorbed layer into the diffused layer, arrow 3 shows the protons diffusing from the diffused layer into the aqueous bulk phase, arrow 4 shows the protons diffusing from the aqueous bulk phase into the diffused layer; and arrow 5 shows protons diffusing from the diffused layer into the absorbed layer.

the green QD biosensors have a negligible influence on the fluorescent intensity of orange QD biosensors. On the basis of this primary model, more than three different kinds of QDs could be mixed together to construct multicolor QD biosensors, which may be a feasible method to optical encoding detection of various viruses in the future.

Conclusions

In summary, we demonstrated that the green and orange pH-sensitive CdTe QDs could be used as the convenient, cheap, reversible, and effective fluorescent probes to monitor the proton flux driven by ATP synthesis for dual simultaneous and independent detection of viruses based on the antibody−antigen reactions. A new QD biosensor fluorescent measurement system was established for rapid, simultaneous, and independent detection of H9 avian influenza virus and MHV68 virus. To describe the mechanism of the QD-based biosensors, a steady electric double layer model has been established to illustrate the mechanism of simultaneous and independent detection of the QD biosensors. The methods described in this paper are of not only theoretical value, but also technical significance, which is also an indispensable and significant step toward optical encoding detection. It is expected that the QD biosensors can be flexible enough to extend to detection of other biomolecules beside viruses and have a great potential for optical encoding used in simultaneous and independent multicolor qualitative and quantitative detection systems.

Acknowledgment. We thank Prof. Kechun Lin in Peking University for the help in English. The current investigations are financially supported by the Hi-Tech Research and Development Program of China (863) (Grant 2006AA03Z327), National Natural Science Foundation of China (Grant 20645003, 30292905, 30490174, and 60372009), and nanobiomedical and device applications of CAS (Grant No. Kjcx-sw-h12).

Supporting Information Available: XRD and SAED patterns of CdTe QDs, quantification of the CdTe QDs on the surface of the chromatophores, the relationship between the fluorescence intensity and synthesis/hydrolysis of CdTe QD chromatophores, and the measurement of F_0F_1-ATP synthase activity using different systems. This material is available free of charge via the Internet at http://pubs.acs.org.

References and Notes

(1) Bruchez, M.; Morrone, P.; Gin, S.; Weiss, S.; Alivisatos, A. P. *Science* **1998**, *281*, 2013−2016.
(2) Chan, W. C.; Nie, S. *Science* **1998**, *281*, 2016−2018.
(3) Dubertret, B.; Skourides, P.; Norris, D. J.; Noireaux, V.; Brivanlou, A. H.; Libchaber, A. *Science* **2002**, *298*, 1759−1762.
(4) Wu, X. Y.; Liu, H. J.; Liu, J. Q.; Haley, K. N.; Treadway, J. A.; Larson, J. P.; Ge, N. F.; Peale, F.; Bruchez, M. P. *Nat. Biotechnol.* **2003**, *21*, 41−46.
(5) Gao, X.; Cui, Y.; Levenson, R. M.; Chung, L. W.; Nie, S. *Nat. Biotechnol.* **2004**, *22*, 969−976.
(6) Bakalova, R.; Ohba, H.; Zhelev, Z.; Ishikawa, M.; Baba, Y. *Nat. Biotechnol.* **2004**, *22*, 1360−1361.
(7) Mattoussi, H.; Mauro, J. M.; Goldman, E. R.; Anderson, G. P.; Sundar, V. C.; Mikulec, F. V.; Bawendi, M. G. *J. Am. Chem. Soc.* **2000**, *122*, 12142−12150.
(8) Gao, X. H.; Nie, S. M. *J. Phys. Chem. B* **2003**, *107*, 11575−11578.
(9) Gao, X.; Nie, S. *Anal. Chem.* **2004**, *76*, 2406−2410.
(10) Pinaud, F.; King, D.; Moore, H.-P.; Weiss, S. *J. Am. Chem. Soc.* **2004**, *126*, 6115−6123.
(11) Medintz, I. L.; Uyeda, T.; Goldman, E.; Mattoussi, H. *Nat. Mater.* **2005**, *4*, 435−446.
(12) Michalet, X.; Pinaud, F. F.; Bentolila, L. A.; Tsay, J. M.; Doose, S.; Li, J. J.; Sundaresan, G.; Wu, A. M.; Gambhir, S. S.; Weiss, S. *Science* **2005**, *307*, 538−544.
(13) Zhelev, Z.; Bakalova, R.; Ohba, H.; Jose, R.; Imai, Y.; Baba, Y. *Anal. Chem.* **2006**, *78*, 321−330.
(14) Kim, S.; Bawendi, M. G. *J. Am. Chem. Soc.* **2003**, *125*, 14652−14653.
(15) Wang, Y. A.; Li, J. J.; Chen, H.; Peng, X. *J. Am. Chem. Soc.* **2002**, *124*, 2293−2298.
(16) Peng, Z. A.; Peng, X. *J. Am. Chem. Soc.* **2001**, *123*, 183−184.
(17) Deng, Z. T.; Cao, L.; Tang, F. Q.; Zou, B. S. *J. Phys. Chem. B* **2005**, *109*, 16671−16675.
(18) Goldman, E. R.; Clapp, A. R.; Anderson, G. P.; Uyeda, H. T.; Mauro, J. M.; Medintz, I. L.; Mattoussi, H. *Anal. Chem.* **2004**, *76*, 684−688.
(19) Hahn, M. A.; Tabb, J. S.; Krauss, T. D. *Anal. Chem.* **2005**, *77*, 4861−4869.
(20) Bakalova, R.; Zhelev, Z.; Aoki, I.; Ohba, H.; Imai, Y.; Kanno, I. *Anal. Chem.* **2006**, *78*, 5925−5932.
(21) Gao, M. Y.; Kirstein, S.; Möhwald, H.; Rogach, A. L.; Kornowski, A.; Eychmüller, A.; Weller, H. *J. Phys. Chem. B* **1998**, *102*, 8360−8363.
(22) Gaponik, N.; Talapin, D. V.; Rogach, A. L.; Hoppe, K.; Shevchenko, E. V.; Kornowski, A.; Eychmueller, A.; Weller, H. *J. Phys. Chem. B* **2002**, *106*, 7177−7185.
(23) Shavel, A.; Gaponik, N.; Eychmuller, A. *J. Phys. Chem. B.* **2006**, *110*, 19280−19284.
(24) Snee, P. T.; Somers, R. C.; Nair, G.; Zimmer, J. P.; Bawendi, M. G.; Nocera, D. G. *J. Am. Chem. Soc.* **2006**, *128*, 13320−13321.
(25) Tomasulo, M.; Yildiz, I.; Raymo, F. M. *J. Phys. Chem. B.* **2006**, *110*, 3853−3855.
(26) Boyer, P. D. *Annu. Rev. Biochem.* **1997**, *66*, 717−749.
(27) Fillingame, R. H. *J. Exp. Biol.* **1997**, *200*, 217−224.

(28) Liu, X. L.; Zhang, X. A., Cui, Y. B; Yue, J. C.; Luo, Z. Y.; Jiang, P. D. *Biochem. Biophys. Res. Commun.* **2006**, *347*, 752−757.
(29) Liu, X. L.; Zhang, Y.; Yue, J. C.; Jiang P. D.; Zhang Z. X. *Biochem. Biophys. Res. Commun.* **2006**, *342*, 1319−1322.
(30) Zhang, Y.; Deng, Z. T.; Yue, J. C.; Tang, F. Q.; Wei, Q. *Anal. Biochem.* **2007**, *364*, 122−127.
(31) Han, M. Y.; Gao, X. H.; Su, J. Z.; Nie, S. *Nat. Biotechnol*. **2001**, *19*, 631−635.
(32) Gromet-Elhanan, Z.; Khanashvili, D. *Methods Enzymol*. **1986**, *126*, 528−538.
(33) Philosoph, S.; Binder, A.; Gromet-Elhanan, Z. *J. Biol. Chem.* **1977**, *252*, 8747−8752.
(34) Montemagno, C.; Bachand, G. D. *Nanotechnology* **1999**, *10*, 225−231.
(35) Zhang, Y. H.; Wang, J.; Cui, Y. B.; Yue, J. C.; Fang, X. H. *Biochem. Biophys. Res. Commun.* **2005**, *331*, 370−374.
(36) Hanley, W. C.; Artwohl, J. E.; Bennett, B. T. *ILAR J.* **1995**, *37*, 93−118.
(37) Burda, C.; Chen, X.; Narayanan, R.; El-Sayed, M. A. *Chem. Rev.* **2005**, *105*, 1025−1102.
(38) Wuister, S. F.; Swart, I.; Driel, F. V.; Hickey, S. G.; de M. Donega, C. *Nano Lett.* **2003**, *3*, 503−507.
(39) Zhang, H.; Zhou, Z.; Yang, B.; Gao, M. Y. *J. Phys. Chem. B* **2003**, *107*, 8−13.
(40) Lei, Y.; Jiang, C. Y.; Liu, S. J.; Miao, Y. M.; Zou, B. S. *J. Nanosci. Nanotechnol.* **2006**, *6*, 3784−3788.
(41) Shapovalov, V. L.; Ryskin, M. E.; Konovalov, O. V.; Hermelink, A.; Brezesinski, G. *J. Phys. Chem. B* **2007**, *111*, 3927−3934.
(42) Hurth, C.; Li, C.; Bard, A. J. *J. Phys. Chem. C* **2007**, *111*, 4620−4627.
(43) Yang, K. L.; Yiacoumi, S.; Tsouris, C. *Nano Lett.* **2002**, *2*, 1433−1437.